AGU PUBLICATIONS

Global Biogeochemical Cycles

RESEARCH ARTICLE
10.1002/2013GB004794

Key Points:
- Atmospheric N, P, and Fe deposition estimated for West Pacific
- Deposition is P deficient relative to Redfield and lower than Atlantic
- Deposition increases primary production by 10%, mainly by N2 fixation

Correspondence to:
T. D. Jickells,
T.Jickells@uea.ac.uk

Citation:
Martino, M., D. Hamilton, A. R. Baker, T. D. Jickells, T. Bromley, Y. Nojiri, B. Quack, and P. W. Boyd (2014), Western Pacific atmospheric nutrient deposition fluxes, their impact on surface ocean productivity, *Global Biogeochem. Cycles*, *28*, 712–728, doi:10.1002/2013GB004794.

Received 13 DEC 2013
Accepted 11 JUN 2014
Accepted article online 13 JUN 2014
Published online 15 JUL 2014

Western Pacific atmospheric nutrient deposition fluxes, their impact on surface ocean productivity

M. Martino[1], D. Hamilton[1], A. R. Baker[1], T. D. Jickells[1], T. Bromley[2], Y. Nojiri[3], B. Quack[4], and P. W. Boyd[5,6]

[1]Centre for Ocean and Atmospheric Sciences, University of East Anglia, Norwich, UK, [2]National Institute of Water and Atmosphere, Wellington, New Zealand, [3]National Institute for Environmental Studies, Tsukuba, Japan, [4]Helmholtz-Zentrum für Ozeanforschung Kiel (GEOMAR), Marine Biogeochemie/Chemische Ozeanographie, Kiel, Germany, [5]NIWA Centre for Chemical and Physical Oceanography, Department of Chemistry, University of Otago, Dunedin, New Zealand, [6]Now at Institute for Marine and Antarctic Studies, University of Tasmania, Hobart, Tasmania, Australia

Abstract The atmospheric deposition of both macronutrients and micronutrients plays an important role in driving primary productivity, particularly in the low-latitude ocean. We report aerosol major ion measurements for five ship-based sampling campaigns in the western Pacific from ~25°N to 20°S and compare the results with those from Atlantic meridional transects (~50°N to 50°S) with aerosols collected and analyzed in the same laboratory, allowing full incomparability. We discuss sources of the main nutrient species (nitrogen (N), phosphorus (P), and iron (Fe)) in the aerosols and their stoichiometry. Striking north–south gradients are evident over both basins with the Northern Hemisphere more impacted by terrestrial dust sources and anthropogenic emissions and the North Atlantic apparently more impacted than the North Pacific. We estimate the atmospheric supply rates of these nutrients and the potential impact of the atmospheric deposition on the tropical western Pacific. Our results suggest that the atmospheric deposition is P deficient relative to the needs of the resident phytoplankton. These findings suggest that atmospheric supply of N, Fe, and P increases primary productivity utilizing some of the residual excess phosphorus (P*) in the surface waters to compensate for aerosol P deficiency. Regional primary productivity is further enhanced via the stimulation of nitrogen fixation fuelled by the residual atmospheric iron and P*. Our stoichiometric calculations reveal that a P* of 0.1 μmol L^{-1} can offset the P deficiency in atmospheric supply for many months. This study suggests that atmospheric deposition may sustain ~10% of primary production in both the western tropical Pacific.

1. Introduction

Primary productivity is primarily limited by the availability of nutrients (macro- and micro-) and light within the surface ocean. Atmospheric supply of both macronutrients and micronutrients therefore plays an important role in setting primary productivity in some ocean areas [*Ward et al*., 2013; *Moore et al*., 2013]. Specifically, nitrogen [*Duce et al*., 2008], iron [*Jickells et al*., 2005], and phosphorus [*Mahowald et al*., 2008] can individually enhance primary productivity, but to fully understand the effects of atmospheric deposition, it is important to consider these three nutrients together [e.g., *Baker et al*., 2003; *Okin et al*., 2011; *Ward et al*., 2013]. Knowledge of the stoichiometry of nutrient supply from aerosols can then be compared with the stoichiometry of ambient surface ocean nutrients and the stoichiometric requirements of the resident phytoplankton [*Boyd et al*., 2010; *Moore et al*., 2013] to estimate the impact of the atmospheric deposition on phytoplankton primary production.

Nitrogen, iron, and phosphorus have diverse sources to the atmosphere. Nitrogen is mainly released by anthropogenic emissions from agriculture (as reduced nitrogen, ammonium) and combustion processes (as nitrogen oxides, which are processed in the atmosphere to yield nitric acid and nitrate) plus an organic nitrogen fraction of rather uncertain origin [*Duce et al*., 2008; *Cape et al*., 2011]. Iron and phosphorus are associated with crustal dust and, to a lesser extent, anthropogenic and (for P) biogenic sources [*Jickells et al*., 2005; *Mahowald et al*., 2008; *Sholkovitz et al*., 2012].

There have been numerous studies of atmospheric aerosol concentrations over the Pacific Ocean, particularly the North Pacific, including studies of dust and iron transport [*Uematsu et al*., 2003; *Matsumoto et al*., 2004;

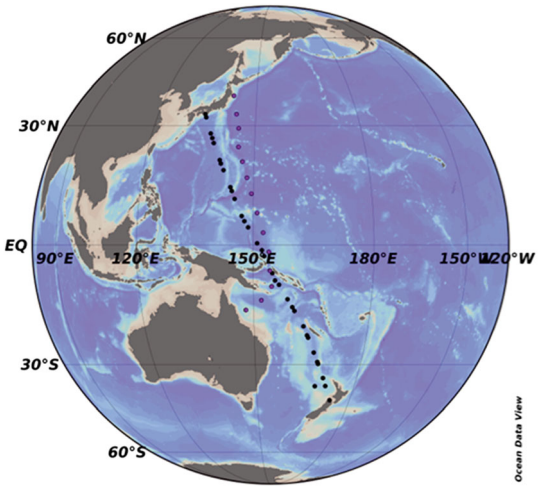

Figure 1. Sample start positions for the four Transfuture 5 (TF5) (black dots) and TransBrom (purple dots) cruises. Cruise dates were as follows: TF5-1 May/June 2007, TF5-2 April/May 2008, TF5-3 August/September 2008, TF5-5 October/ November 2009, and TransBrom October 2009.

Moffet et al., 2012, *Prospero et al*., 1989, *Wagener et al*., 2008], nitrogen [*Savoie et al*., 1989; *Jung et al*., 2011; *Nakamura et al*., 2006; *Miyazaki et al*., 2010; *Miyazaki et al*., 2011; *Zhang et al*., 2011; *Ooki et al*., 2007], as well as contaminants [*Uematsu et al*., 2010; *Moffet et al*., 2012] but fewer studies of phosphorus [*Furutani et al*., 2010; *Hsu et al*., 2010]. Together, these studies emphasize the general patterns of atmospheric transport over the Pacific (discussed further below) with high concentrations of dust (and associated iron), anthropogenically derived metals and nitrogen in the Asian plume passing over the NW Pacific, particularly in spring. Much lower concentrations of all these components are found over the central and South Pacific, and particularly low concentrations in the SE Pacific. Despite this rich literature on atmospheric deposition, many of these studies focused only on individual nutrients, and somewhat different methods have been used to estimate atmospheric nutrient supply. This can complicate the task of comparing trends in atmospheric deposition between ocean basins, and for the assessment of the N:P:Fe stoichiometry of atmospherically supplied nutrients.

The biological effects of atmospheric deposition depends both on the magnitude of atmospheric deposition and on the biogeochemical signature of the receiving waters. In surface ocean waters that are deficient in particular nutrients, atmospheric deposition of these deficient nutrients can directly stimulate primary production by alleviating this limitation, something that has been inferred to take place with nitrogen deposition to tropical waters and iron deposition to high-nutrient, low-chlorophyll waters [*Duce et al*., 2008; *Jickells et al*., 2005]. In some ocean areas, nitrogen fixation has been suggested to be a particularly important source of nitrogen for the phytoplankton community [e.g., *Moore et al*., 2013]. Nitrogen fixation, a key process in the global nitrogen cycle and a mechanism by which phytoplankton communities can escape from nitrogen limitation, requires both iron and phosphorus [*Mills et al*., 2004]. Hence, atmospheric iron supply may play a pivotal role in regulating nitrogen fixation along with the utilization of excess phosphorus in surface waters to meet phosphorus requirements [e.g., *Mahaffey et al*., 2005; *Kitajima et al*., 2009; *Behrenfeld et al*., 2009; *Somes et al*., 2010; *Dutkiewicz et al*., 2012; *Ward et al*., 2013].

Atmospheric deposition in the Atlantic is strongly P deficient relative to phytoplankton requirements [*Baker et al*., 2003, 2010], and models suggest that this is the case over most ocean areas [*Okin et al*., 2011]. Over the Atlantic Ocean, strong north (high) to south (low) gradients in the atmospheric deposition of both iron and nitrogen (ammonium + nitrate + organic nitrogen) lead to gradients in the influence of atmospheric deposition on rates of primary production and nitrogen fixation [*Baker et al*., 2003]. The iron deposition has been shown to result in the stimulation of nitrogen fixation in the tropical North Atlantic leading to extreme surface water phosphorus depletion [*Moore et al*., 2009; *Ward et al*., 2013], and low (~0.1 μmol L^{-1}) values of P* (the excess of phosphorus relative to nitrate compared to Redfield stoichiometry [*Deutsch et al*., 2007], indicating surface waters with a relatively small excess of phosphorus relative to phytoplankton requirements. The tropical western Pacific is a region of generally low ambient surface concentrations of essential phytoplankton nutrients (nitrogen, phosphorus, and iron) and low rates of primary productivity [*Deutsch et al*., 2007; *Ward et al*., 2013; *Behrenfeld et al*., 2009]. P* values in the surface waters of the western Pacific increase from 0.1 μmol L^{-1} in the north to 0.2 μmol L^{-1} in the south, indicating a north-to-south increase in P availability relative to N [*Deutsch et al*., 2007]. The potential importance of atmospheric nitrogen deposition in setting rates of primary production in this region has been reported [*Kim et al*., 2011].

Here we consider the West Pacific (Figure 1), focusing particularly on the tropical region and report data for aerosol nitrogen and phosphorus concentrations, together with aerosol dust and iron concentrations estimated from non-sea-salt (nss) calcium. We use these data sets to investigate the biogeochemical and

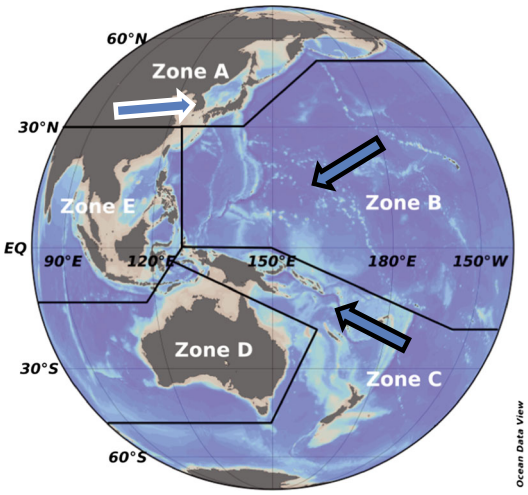

Figure 2. Classification of air mass back trajectory zones. Zone A: Asia. Zone B: Open Pacific. Zone C: Indonesia/Micronesia/New Zealand and Southern Ocean. Zone D: Australia. Zone E: Southern Asia. Main air flow regimes of relevance to this paper are indicated.

stoichiometric effects of the concurrent deposition of these nutrients on Pacific marine biogeochemistry using comparable approaches to those we employed in the Atlantic Ocean [*Baker et al*., 2003].

2. Aerosol Climatology of the Western Pacific

Given its importance to subsequent data interpretation, we begin by briefly describing the climatology of atmospheric transport over the Pacific. We later discuss the results of air mass back trajectory analysis for individual aerosol samples collected which can then be compared to the average climatology.

The atmospheric climatology of the Pacific and the associated transport of aerosols were first comprehensively described in publications from the sea/air exchange SEAREX program [*Merrill*, 1989]. Emissions from the Asian continent are generally entrained within a westerly flow over the North Pacific. This flow can turn southward moving around the North Pacific subtropical high-pressure system and bringing Asian emissions into the tropical central Pacific region within the northeast trade winds. The merger of moisture-laden trade winds in the tropical Pacific leads to the formation of the convergence zones (CZs) [*Merrill*, 1989]. The intertropical convergence zone (ITCZ) of the equatorial North Pacific is the most persistent of the convergences in the Pacific Ocean lying between 2 and 12°N, crossing the breadth of the Pacific Ocean, and forming a strong barrier to interhemisphere transport. The ITCZ and South Pacific Convergence Zone (SPCZ) merge together in an area of the Western Pacific called the warm pool, but farther east, they separate with the SPCZ extending to the southeast toward the southern tropics and finally the open South Pacific Ocean. The boundaries of zones B and C and C and D in Figure 2 approximate to the ITCZ and SPCZ, respectively, although the exact positions are seasonally variable. The main air flow patterns discussed above that are relevant to our data sets are also shown schematically in Figure 2.

The constant deep atmospheric convection and high precipitation rates associated with the convergence zones make accurate back trajectory analysis difficult once the wind has entered a CZ [*Merrill*, 1989]. The SPCZ is thought to form a weaker transport barrier than the ITCZ. It fluctuates in strength seasonally, with major atmospheric circulation changes associated with El Niño–Southern Oscillation events, and may also be sensitive to future climate change [*Cai et al*., 2012]. The atmospheric transport paths in the South Pacific are less well understood than those in the North Pacific. In the equatorial SW Pacific region sampled in the work reported here, the climatological atmospheric flow is from the SE associated with the south easterly trade winds. South of the SPCZ (~10°S for the ocean regions covered by the sampling campaigns considered here) the air flow is predominantly from the south including transport from the SW which may cross Australia.

Dust is a useful tracer for continental aerosol over the North Pacific with the main dust sources being in Northern China [*Xuan and Sokolik*, 2002]. The strength of dust transport from the region is determined by the amount of dust entering the westerly air stream above Asia, particularly influenced by dust storms, and the acceleration of winds toward western North America [*Song et al*., 2008] which, together with low rainfall, contributes to a seasonal maximum in dust transport in the spring [*Xuan and Sokolik*, 2002; *Merrill et al*., 1985; *Merrill*, 1989; *Natsagdorj et al*., 2003]. Westerly flows carry this dust over areas of major anthropogenic emissions from China and eastward toward the North Pacific, where at least some of this material is deposited [e.g., *Prospero et al*., 1989; *Huebert et al*., 2003; *Arimoto et al*., 2004; *Uematsu et al*., 2003]. Although the equatorial Pacific region under the influence of the north easterly trade winds has much lower dust concentrations, the SEAREX program reported a small spring increase in dust concentrations over the central equatorial Pacific derived from Asian desert sources. The estimated transit times from the Asian continent to the tropical North Pacific island sites, such as Enewetak, was of the order of 10 days [*Merrill*, 1989]

with much of the continental aerosol lost from the air mass by mixing and deposition during transport. North American emissions can also become entrained within these easterly trade wind flows [*Merrill*, 1989]. In the South Pacific the dominant dust source is the Australian continent, and the dust is mainly transported either westerly toward the Indian Ocean, or south easterly toward the Southern Ocean and as far as Antarctica [*Revel-Rolland et al*., 2006], and hence does not usually cross our sampling route. This pattern of dust emission and transport leads to a strong gradient in dust deposition over the Pacific with high concentrations over the NW Pacific and a strong interhemispheric gradient over much of the Pacific although, in the western Pacific, models suggest similar deposition rates to those seen in the North Pacific [e.g., *Jickells et al*., 2005].

3. Methods

3.1. Sampling

The data presented here were collected on four campaigns (labeled here as TF5-1, 2, 3, and 5) by scientists on board the commercial vessel *Transfuture 5* operating between Nelson (New Zealand) and Osaka (Japan) as part of the Ship of Opportunity program of the Centre for Global Environment Research of the National Institute for Environmental Studies, Ibaraki, Japan led by Nojiri (http://soop.jp/index.html) [*Nara et al*., 2011]. Samples were also collected during the TransBrom campaign on board the RV *Sonne* from Tomakomai (Japan) to Townsville (Australia) [*Krüger and Quack*, 2013]. The campaigns all followed a similar route, although TransBrom traveled in a southerly direction and only as far as 14.5°S (Figure 1).

Aerosol sampling procedures were similar to those described previously [*Baker et al*., 2006a]. The aerosol samples were collected onto Whatman 41 cellulose filter paper using a high-volume (TF5 ~ 48 $m^3 h^{-1}$; TransBrom ~ 66 $m^3 h^{-1}$) aerosol collector. Sampling was usually for 1 (24 h) day. The average speed of Transfuture 5 is 35.5 $km h^{-1}$, so samples are collected over ~ 852 km of voyage track. There was no sector control employed on the aerosol sampler, as it was deployed ~40 m forward of the location of the ship's emissions, and at these speeds we consider contamination from ship emissions to be highly unlikely, and there is no evidence for such contamination in any of our data. To test this further, it is possible to interrogate the 10 min average of the continuous atmospheric CO_2 sampling system on board the *Transfuture* (http://soop.jp/) to evaluate the potential for contamination from ship-based sources, assuming these would give rise to elevated and variable CO_2 concentrations. Such variability in CO_2 is periodically evident in the data set but is most commonly associated with the ship passing relatively close to islands in the Tongan arc region where we see other evidence to suggest that volcanic sources are important as discussed later. Otherwise, the variability in atmospheric CO_2 concentrations recorded is small and does not appear to be associated with anomalies in aerosol concentrations, suggesting no ship-based contamination of the aerosol samples. We therefore retain all of the data and evaluate later if the results are consistent with other published data.

The sampling on the RV *Sonne* was similarly arranged to avoid any influence of ship emissions. The speed of this research ship was much less than the commercial vessel Transfuture 5 and distances traveled during daily sampling (average ~400 km) were therefore less. Sampling was routinely monitored by ship board scientific personnel to ensure no possibility of contamination from ship sources, with sampling stopped if apparent wind direction became such as to threaten contamination. A Sierra-type cascade impactor was employed for TransBrom to separate the aerosol into coarse and fine modes at a boundary of ~1 μm aerodynamic diameter [*Baker et al*., 2006a], whereas the TF5 cruises used bulk filter collection only.

3.2. Analysis

The analysis methods used are only summarized here, with full details being reported previously [e.g., *Baker et al*., 2007, 2006a; *Yeatman et al*., 2001]. Extraction of the aerosol from the filter paper was in ultrapure water (Purite 18.2MΩ) for most components and 1 mM $NaHCO_3$ solution for phosphorus, via ultrasonic agitation for 1 h, followed by filtration (minisart) at 0.2 μm. Analytical methods are summarized in Table 1.

Blank filters were analyzed and all results reported are blank corrected. Overall detection limits are shown in Table 2. When samples were below detection, a situation that occurred for some phosphorus analyses ($n = 4$) and for almost no other analytes, 75% of the detection value was used as a concentration for samples below the limit of detection (lod) for averaging purposes. Because these lod results were only a small proportion of the total data set, this substitution has very little effect on the median values we report. In Table 2 and subsequently we focus on the key nutrient analytes of interest and hence do not report the results for sodium, chloride, or magnesium

Table 1. Extraction and Analysis Methods Employed for Analysis of Various Aerosol Components

Analyte	Extract	Analysis[a]
Major cations[b]	Ultra pure water	ICP-OES
Major anions[c]	Ultra pure water	IC
NH_4^+	Ultra pure water	AA
Total soluble nitrogen	Ultra pure water	HT Cat. Ox.
Soluble phosphorus	1 mM $NaHCO_3$, pH 7	Spectroph.

[a]ICP-OES-inductively coupled plasma-optical emission spectroscopy; IC-ion chromatography; AA-auto analyzer using the indophenol blue reaction; HT Cat. Ox.-high temperature catalytic oxidation; Spectroph.-spectrophotometry.
[b]Major cations-Na^+, Ca^{2+}, Mg^{2+}, K^+.
[c]Major anions-Cl^-, SO_4^{2-}, NO_3^-.

concentrations. Our analysis methods only measure phosphate and related soluble and reactive forms of phosphorus, subsequently referred to as soluble inorganic phosphorus (SIP). *Baker et al.* [2006b] estimate that SIP is about one third of total P, and *Furutani et al.* [2010] report a similar distribution. Much of the remaining phosphorus may be bound to organic matter of uncertain bioavailability or tightly bound within mineral phases such as aluminosilicate lattices and hence probably not bioavailable. Phosphorus was not analyzed on the samples from the TransBrom cruise.

We also report the water soluble organic nitrogen component of our aerosol extracts, WSON, as the difference between measurements of total soluble N and the inorganic N measured as nitrate and ammonium [*Cape et al.*, 2001], i.e.,

$$\mathrm{WSON} = \mathrm{TN} - (\mathrm{NO_3^-} + \mathrm{NH_4^+})$$

WSON concentration estimates can have a relatively large uncertainty and even negative concentrations associated with the compounded uncertainties from using three analytical results in its calculation [*Cape et al.*, 2011; *Cornell et al.*, 2003; *Lesworth et al.*, 2010]. However, in this data set, we only had two negative WSON concentrations in 52 results and we therefore utilize the entire WSON data set available.

We use nss-K^+ as a tracer for biomass burning [e.g., *Allen and Miguel*, 1995], nss-Ca^{2+} as a tracer for mineral dust [e.g., *Kline et al.*, 2004], and non-sea-salt sulphate (SO_4^{2-}) as a tracer of volcanic, biogenic, and anthropogenic sulphur emissions, as discussed below. For these tracers we report the nss concentrations [*Keene et al.*, 1986] using Na^+ as the sea-salt tracer and seawater major ion composition [*Stumm and Morgan*, 1996]. As with WSON, these derived non-sea-salt concentrations have increased analytical uncertainties, but for nss-SO_4^{2-} we report no negative values and for nss-Ca^{2+} only three in 52, while for nss-K^+, where concentrations are rather low, we find five negative concentrations in 52. We retain all negative values when calculating descriptive statistics in order to avoid a positive bias in average concentrations. As with the inclusion of lod estimates described above, the low number of negative values in our data sets will lead to very little effect on the medians of these populations and we therefore consider medians to be more reliable than arithmetic means. We use nss-Ca^{2+} to estimate concentrations of dust and soluble Fe, as described below.

Air mass origin for the samples collected was assessed using 5 day air mass back trajectories obtained from the NOAA Hybrid Single-Particle Lagrangian Integrated Trajectory model [*Draxler and Rolph*, 2003].

Table 2. Aerosol Collection Substrate Blank Values and Limits of Detection[a] for Aerosol Soluble Nutrient and Selected Tracer Species

	Substrate Blanks (nmol/filter)				Detection Limits (nmol m^{-3})			
Analyte	TF5-1 and 2	TF5-3	TF5-5	TransBrom	TF5-1 and 2	TF5-3	TF5-5	TransBrom
NO_3^-	190	153	530	280[b] <110[c]	0.03	0.05	0.43	0.09[b] 0.10[c]
NH_4^+	1100	1110	2890	3400[b] 530[c]	0.18	0.11	1.73	0.28[b] 0.15[c]
TN	2390	2230	2600	6400[b] <4200[c]	0.31	0.19	1.83	1.68[b] 3.74[c]
PO_4^{3-}	14	10	14	nd[d]	0.004	0.003	0.008	nd[d]
Na^+	3030	3100	2900	2400[b] 1500[c]	0.36	0.54	0.32	0.69[b] 0.68[c]
Ca^{2+}	189	181	289	510[b] 510[c]	0.02	0.05	0.15	0.08[b] 0.33[c]
SO_4^{2-}	540	530	550	140[b] 57[c]	0.03	0.03	0.03	0.04[b] 0.17[c]
K^+	100	102	240	80[b] 64[c]	0.03	0.05	0.19	0.04[b] 0.04[c]

[a]Calculated using 3σ of the blank and an assumed equivalent air volume of 1100 m^3 for TF5 and 1500 m^3 for TransBrom (sampling times of ~24 h and 23 h, respectively).
[b]Fine mode.
[c]Coarse mode.
[d]Not determined.

Wet and dry atmospheric deposition rates depend on aerosol particle size. We use the average aerosol size distribution for each species (discussed below) together with deposition velocities of 0.1 cm s^{-1} and 2 cm s^{-1} for fine and coarse mode aerosol, respectively, [*Baker et al*., 2003] to derive a weighted average deposition velocity for each nutrient and multiply this by the median aerosol concentration to estimate the dry deposition flux (F^D).

We estimate wet deposition using scavenging ratios (S) of 240 for ammonium (predominantly fine mode) and 358 for nitrate (predominantly coarse mode) based on an average of Bermuda and Barbados scavenging ratios [*Galloway et al*., 1993]. For WSON and dust which are 45% fine mode, we use a weighted average of the scavenging ratios (i.e., $0.45 \times 240 + 0.55 \times 358 = 305$). We do not have water soluble inorganic phosphorus particle size distributions for these West Pacific aerosols, but we assume it is similar to WSON and dust, as it is in the Atlantic [*Baker et al*., 2010]. Scavenging ratios are then used to calculate rainfall concentrations from aerosol concentrations (C_A) which are converted to wet deposition using a density of air of 1.17 kg m^{-3} [*Galloway et al*., 1993] and an estimated rainfall rate (P) of 4 mm d^{-1}, derived from maps of long-term average precipitation [*Xie and Arkin*, 1997], although we note that rainfall is higher within the ITCZ itself. Hence, we estimate wet deposition flux (F^W) from the equation

$$F^W = [(C_A \times S)/1.17] \times P.$$

4. Results and Discussion

4.1. Atmospheric Transport Paths Sampled

To synthesize the data collected we have used air mass back trajectories to help describe the area over which the air has passed 5 days prior to being sampled. The trajectories were taken at 12 h intervals to give an indication of the air at both the middle sampling point as well as the start/end of each sampling interval. These trajectories were then used to classify the samples according to their likely aerosol source regions.

We selected five potential air mass back trajectory origin classifications A–E (Figure 2) based on climatologies discussed in section 2. However, in practice we sampled no air masses associated with zone E and only two air masses sampled had approached the Australian continent (zone D). In neither case did these trajectories traverse the central desert regions of Australia, and we have therefore included these two samples within trajectory class C to avoid creating trajectory groupings with very small numbers of samples. The major air transport pathways and the trajectories for samples collected allow us to therefore identify three distinct zones:

1. Zone A: Air flows associated with eastward flow off the Asian continent with the potential to be influenced by industrial and domestic emissions and Asian dust sources.
2. Zone B: Air flows in a westerly direction over the tropical Pacific Ocean toward SE Asia associated with the NE trade winds. These air masses have spent many days over the open ocean, but as discussed in the earlier climatology section, long-range transport from Asian and North American sources can reach this region.
3. Zone C: Air flow follows the SPCZ associated with the south easterly trade winds. This air flow has spent many days over the Southern Ocean but may also be influenced by emissions from the Micronesian islands, New Zealand, and coastal Australia.

The air mass back trajectories at particular latitudes were very similar for each voyage and consistent with the climatology of the Pacific described earlier, suggesting that our data should be broadly representative of the region. The major air flows seen in the back trajectories are very similar to those laid out in SEAREX [*Merrill*, 1989], although the air flow from Australia that they described was rarely encountered during the sampling campaigns discussed here, as noted above. Air flowing from zone A was only encountered north of 14°N, and samples with air from zone C were encountered south of 2°S. Although our sampling campaigns took place at different times of year, the number of samples we have collected is too small to allow us to realistically consider seasonality, and so we report statistics for all of the voyages in Table 3. Given the consistency of air mass trajectories, we subsequently treat each zone in Figure 2 as a separate ocean province influenced by air traveling from that region and adjoining continental areas.

Table 3. Average Concentration (Mean, Standard Deviation, and Median All as nmol m^{-3}) for the Various Zones

Zone	NO_3^-	NH_4^+	WSON	SIP[a]	nss-Ca^{2+}	nss-K^+[b]	nss-SO_4^{2-}
A ($n = 9$)							
Median	15	18	7.2	0.058	1.8	0.5	32
Mean	17	21	8.1	0.062	2.4	0.8	26
SD	11	13	5.7	0.046	1.7	0.5	19
B ($n = 21$)							
Median	2.9	7.1	4.3	0.022	0.8	0.4	5.3
Mean	3.9	6.8	4.3	0.041	0.9	0.7	7.1
SD	3.0	3.7	1.7	0.053	0.6	0.8	5.3
C ($n = 22$)							
Median	3.6	7.3	3.5	0.014	0.7	0.6	8.1
Mean	3.8	7.4	3.5	0.018	1.0	0.5	16
SD	2.1	3.2	2.3	0.016	0.8	1.2	22

[a]Zone A $n = 6$, Zone B $n = 15$, Zone C $n = 18$.
[b]nss-K^+ for Zone B $n = 17$.

4.2. Aerosol Average Composition and Comparison to Other Studies

Average concentration results (mean, standard deviation, and median) for the various sectors are presented in Table 3. The mean is included as the majority of other studies in the Pacific report this average value, and hence it is useful for comparisons between data sets which were collected at different times and using slightly different methods.

The size distribution results obtained from the TransBrom samples are consistent with those seen previously in this region [*Matsumoto et al*., 2004] and elsewhere [e.g., *Baker et al*., 2003]. Nitrate was found predominantly in the coarse mode fraction (mean 84% coarse mode) reflecting its association with dust and sea-salt particles. By contrast, aerosol ammonium and non-sea-salt sulphate, which have gas phase precursors, are primarily associated with the fine mode aerosol (mean 75 and 73% fine mode respectively), while WSON and nss-Ca^{2+} both have on average about 45% of their concentration associated with the fine mode. This is similar to the proportions reported by [*Matsumoto et al*., 2004] for nss-Ca^{2+} in this region. WSON was reported to be predominantly associated with fine mode aerosol in samples collected in the NW Pacific using a 2.5 μm size cutoff between fine and coarse modes [*Nakamura et al*., 2006], while others report WSON to be split more or less equally between coarse and fine mode aerosol, in samples collected in Taiwan and over the Atlantic, respectively, for samples collected with a ~1 μm coarse/fine mode cutoff [*Chen et al*., 2010; *Lesworth et al*., 2010]. In the following discussion we report the sum of TransBrom fine and coarse mode concentrations for comparability with the other data.

The nitrate and ammonium concentrations we report here are consistent with other data from the western Pacific and generally higher than those seen farther east (i.e., east of 160°E) in the Pacific [*Jung et al*., 2011]. This lateral gradient is consistent with dilution and deposition of terrestrial-origin aerosol during eastward transport and is also evident in model estimates [e.g., *Duce et al*., 2008]. The concentrations we report here for the air masses crossing zone A are higher than those reported by *Jung et al*. [2011] probably reflecting differences in the magnitude of the impact of industrial emissions from Asian sources on samples of air masses with somewhat different trajectories over that region. Our results are consistent for this region with those from sampling on island stations in the NW Pacific such as Chichi-jima [*Matsumoto et al*., 2004]. In our data, and in the other for this region [*Jung et al*., 2011], aerosol ammonium concentrations are higher than nitrate. *Liu et al*. [2013] have noted that the ammonium/nitrate ratio in atmospheric deposition in China is increasing, reflecting faster growth in ammonia emissions from agriculture than NO_x emissions from combustion sources. Nitrate and ammonium in our data set are well correlated but with a nonzero ammonium intercept (Figure 3), consistent with a background marine ammonia emission [*Jung et al*., 2011]. Sulphate is also well correlated with both nitrate and ammonium, reflecting common sources on the Asian continent.

There is little published data on WSON in this region. The results reported here are higher than those reported for WSON (and nitrate and ammonium) for samples collected farther east than our samples [*Miyazaki et al*., 2011], but lower than those reported from Taiwan [*Chen et al*., 2010] and for the NW Pacific close to Japan [*Nakamura et al*., 2006]. WSON is correlated with TN in our data set,

$$\mathrm{WSON} = 0.16\ (\pm 0.03)\ \mathrm{TN} + 1.6\ (\pm 0.6) \quad R^2 = 0.44\ n = 49$$

suggesting on average about 16% of the total N is WSON, a broadly similar proportion to that found by others in the Pacific region [*Chen et al*., 2010; *Miyazaki et al*., 2011; *Nakamura et al*., 2006] and consistent with that reported for global data sets [*Cape et al*., 2011].

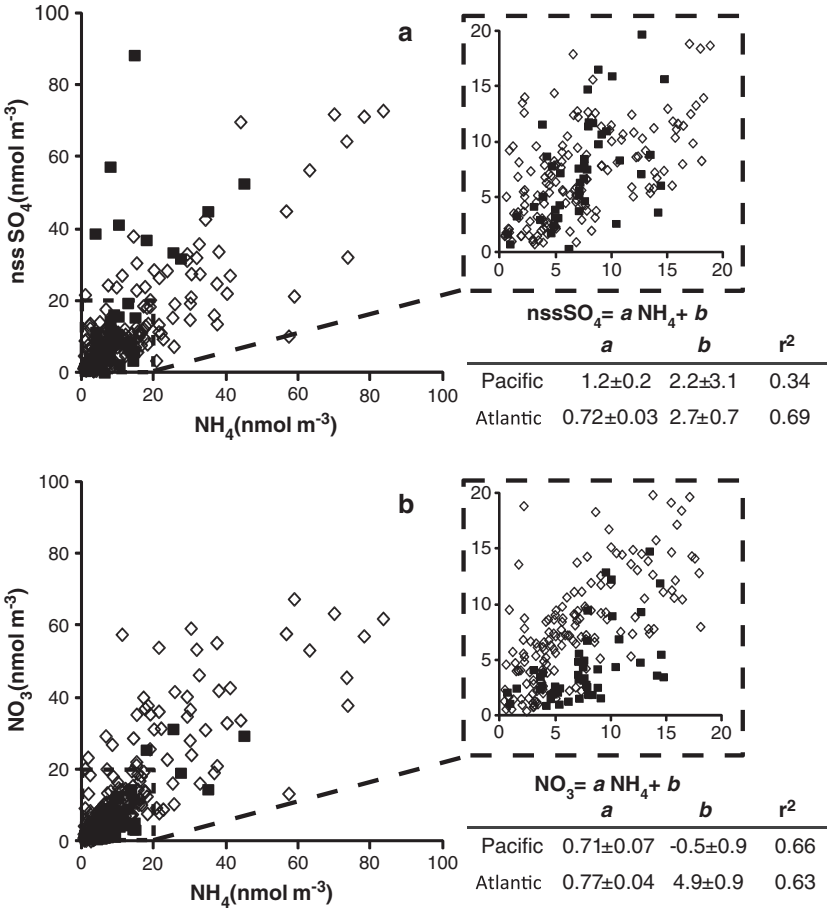

Figure 3. Plots of (a) nss-sulphate and (b) nitrate against ammonium concentrations for the Pacific data presented here (filled squares) and for Atlantic data from *Baker et al.* [2010] (open diamonds). Panels also show enlargements of the lower concentration regions of each plot indicated on the main panels with dashed lines.

The published literature on aerosol phosphorus concentrations is much more limited than for the other components considered here, but we can compare our results to reported average soluble phosphorus concentrations over the central North Pacific of ~0.01 nmol m^{-3} (total P 0.08 nmol m^{-3}) [*Furutani et al.*, 2010]. These values are somewhat lower than the median of our results for air masses from zones B and C. These workers [*Furutani et al.*, 2010] report higher soluble phosphorus concentrations in regions impacted by Asian emissions (average concentration about 0.1 nmol m^{-3}) comparable to, but somewhat higher than, observed here. The aerosol soluble phosphorus concentrations we and others report are very low and approach our detection limits, and hence we do not attempt to interpret the regional variability we see in detail, noting only that the soluble phosphorus concentrations are rather variable and do not correlate particularly well with other aerosol components. It is not straightforward to attribute observed phosphorus concentrations to known sources [*Furutani et al.*, 2010], a finding consistent with the diversity and uncertainty in potential P sources to the atmosphere [*Mahowald et al.*, 2008], although globally dust is the main source. Recent studies over the Bay of Bengal [*Srinivas and Sarin*, 2012], a region strongly impacted by desert dust and anthropogenic emissions, report concentrations of soluble phosphorus more than tenfold greater than those reported here. Clearly, more work is required to understand atmospheric phosphorus transport to the oceans.

Nss-Ca^{2+} has been widely used as a tracer of crustal dust particularly in the Pacific region and also to quantitatively estimate dust concentration [e.g., *Suzuki and Tsunogai*, 1988; *Kline et al.*, 2004; *Arimoto et al.*, 2004]. Such conversions from nss-Ca^{2+} to dust are necessarily uncertain because both the calcium content of dust and its solubility vary. Here we use the approach of *Kline et al.* [2004] who estimated water soluble nss-Ca^{2+} to be 5% of dust by mass in the Asian dust plume. These authors suggest that their

Table 4. Estimated Median Dust Concentrations ($\mu g\,m^{-3}$) in Air Mass Zones Sampled in This Study Compared to Other Literature Values for Long-Term Stations From the Same Region

Zone	All Samples, This Study	Other Published Data, Derived in Part From The Compilation of *Duce* [1995]
A	1.4	NW Pacific 1.7[a], Chinchi-jima 4.4[b], Shemya 0.9[c],
B	0.6	Enewetak 0.3[d], Nauru 0.1[e], West Pacific 1.2[f]
C	0.6	Norfolk Island 0.4[g], New Caledonia 0.2[e]

[a] *Tsunogai and Kondo* [1982].
[b] *Tsunogai et al.* [1985].
[c] *Uematsu et al.* [1983].
[d] *Uematsu et al.* [1983].
[e] *Prospero et al.* [1989].
[f] *Zhou et al.* [1992].
[g] *Duce* [1995].

resulting conversion factor for nss-Ca^{2+} has an uncertainty of at least a factor of 2 [*Kline et al.*, 2004]. Within this uncertainty, this percentage nss-Ca^{2+} is consistent with other estimates from the Pacific region [*Suzuki and Tsunogai*, 1988; *Arimoto et al.*, 2004] and with estimates for the Saharan dust plume [*Savoie and Prospero*, 1980].

The results of these estimates of dust concentrations are presented in Table 4. Although this data set covers a large ocean area, it is necessarily restricted in time and we compare the results to those collected at island stations over campaigns lasting many months or longer to test the representativeness of the data. The nss-Ca^{2+} data we report in zone A are very similar to that reported for Chinchi-jima in the NW Pacific [*Matsumoto et al.*, 2004]. As shown in Table 4, our dust concentration estimates are consistent with the extensive compilation of *Duce* [1995]. There is a general west to east gradient in concentrations in the Pacific reflecting transport distances from the Asian source [e.g., *Uematsu et al.*, 2003; *Jickells et al.*, 2005]. Hence, the dust concentrations we find in the SW Pacific (0.6 $\mu g\,m^{-3}$ zone C) are markedly higher than those reported in the SE Pacific (~10 $ng\,m^{-3}$) [*Wagener et al.*, 2008], while even higher dust concentrations $>20\,\mu g\,m^{-3}$ are found in Zone A near the Japanese coast [*Uematsu et al.*, 2003]. The natural variability of dust concentrations dominates the uncertainties in dust and iron concentrations. To estimate soluble iron flux from the dust flux we assume the dust is 3.5% Fe [*Jickells et al.*, 2005] and an iron solubility of 5% for aerosols which is appropriate for this atmospheric dust loading [*Baker and Jickells*, 2006], and 14% for iron in rainwater [*Jickells and Spokes*, 2001], although these estimates have substantial uncertainties of at least a factor of 2.

4.3. Geographic Pattern of Aerosol Concentrations

The concentrations we report in Tables 3 and 4 conform to a rather simple broad geographic pattern with zone A air masses higher than zones B and C for all components, except nss-SO_4^{2-} as discussed below. The geographical pattern in average dust concentrations we find is entirely consistent with that reported by others in the Pacific [e.g., *Prospero et al.*, 1989] and is likely the result of long-range transport from Asia over the North Pacific and from Australia over the South Pacific [*Prospero et al.*, 1989]. The geographic patterns we report for nitrate and ammonium are also similar to those reported by others [*Jung et al.*, 2011; *Savoie et al.*, 1989; *Ooki et al.*, 2007]. These authors again argue that the distribution of nitrate and ammonium reflects long-range transport from primarily Asian sources overlain on a natural background derived from lightning and tropospheric exchange for aerosol nitrate and marine emissions of ammonia for aerosol ammonium. The consistency of our data and that of Savoie analyzed with similar methods, suggests that increasing Asian emissions in recent decades [e.g., *Liu et al.*, 2013; *Zhang et al.*, 2007] is not yet having a major impact on the central Pacific Ocean region.

The overall pattern we see for nss-SO_4^{2-} is similar to that reported by others, of decreasing concentrations along transport pathways from Asia and Australia with additional sulphate sources from the emissions of dimethyl sulfide from seawater [*Savoie et al.*, 1989; *Ooki et al.*, 2007]. However, our nss-SO_4^{2-} data also show higher-average concentrations in air masses associated with Zone C due to a few samples with particularly high concentrations, among a data set with otherwise low concentrations (see Figure 4); three of 52 samples have nss-SO_4^{2-} concentrations $>40\,nmol\,m^{-3}$ while the remaining samples have concentrations $<15\,nmol\,m^{-3}$. All of the samples with higher nss-SO_4^{2-} concentrations are collected in the northern part of zone C and are associated with trajectories passing over, or close to, the Tongan and Vanuatu islands. We suggest that the high nss-SO_4^{2-} aerosol concentrations in these samples are derived from emissions from the numerous volcanoes in this region. The concentrations of nss-SO_4^{2-} we find in these samples are comparable to those reported for samples influenced by SO_2 emissions from volcanoes in Japan collected in the NW Pacific [*Uematsu et al.*, 2004].

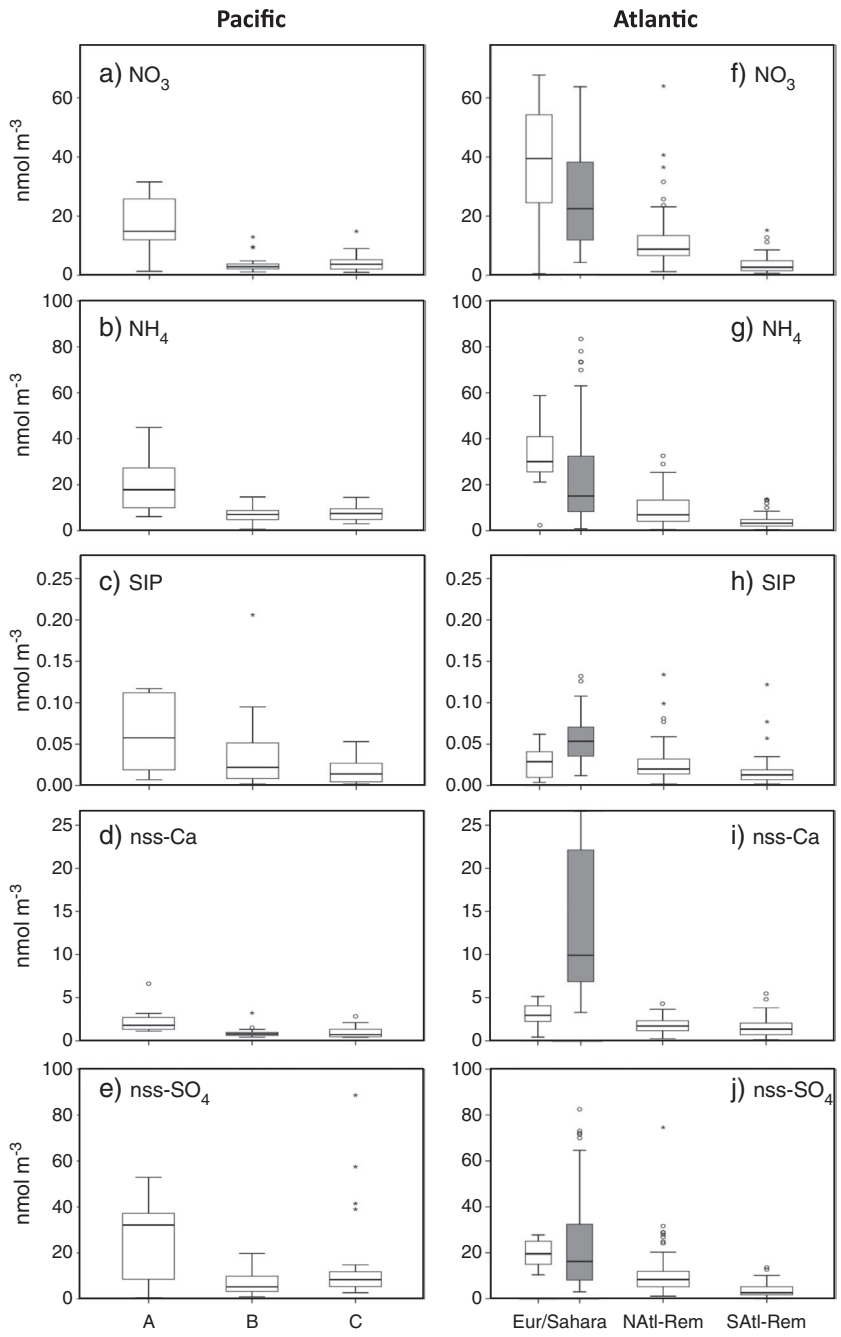

Figure 4. Box and whisker plots showing the distribution of nitrate, ammonium, SIP, nss-Ca and non-sea-salt sulphate (a–e) for zones A, B, and C in the Pacific sampled here. (f–j) Distributions of these species in equivalent air masses sampled in the Atlantic Ocean (data from *Baker et al.* [2010]). Note that two negative points for nss-Ca^{2+} and nss-SO_4^{2-} are excluded from these plots. The Saharan flow regime data are highlighted to aid comparison to other regions.

4.4. Comparison of Aerosol Concentrations Between the West Pacific and the Atlantic Ocean

We have previously reported results of similar sampling of aerosols along an extensive meridional transect in the Atlantic Ocean [e.g., *Baker et al.*, 2006a, 2010, 2006b]. We now compare and contrast the results from those Atlantic transects to those reported here for the western Pacific, recognizing that sample numbers in individual regions for the West Pacific samples are relatively small.

Pacific aerosol samples collected in Zone A in this study are potentially impacted by both dust and anthropogenic emissions from Asian continental regions. We therefore compare Zone A to North Atlantic air

masses influenced by European emissions (Eur, Figure 4) and to air over the subtropical North Atlantic, which is impacted by Sahara desert dust sources and by anthropogenic emissions from North Africa and southern Europe (Sahara, Figure 4). In making this comparison we acknowledge that our transect in the Pacific only passes through a part of the Asian outflow, which extends farther north than our sampling. This, combined with different patterns of emissions, contributes to some of the differences that are evident in Figure 4. The concentrations we report for Zone A samples in the Pacific are lower than that reported for the European outflow, but comparable to the Saharan outflow for nitrate and ammonium, although over the North Atlantic, nitrate to ammonium ratios are about 1.4 while in Zone A samples, they are about 0.8. This reflects the increasing relative importance of NH_3 over NO_x emissions in China compared to the situation in Europe [*Liu et al*., 2013]. Non-sea-salt sulphate concentrations were higher in zone A than in the NAtl-Rem and Eur groups in the Atlantic, probably reflecting different patterns of relative emissions of the nitrate, ammonium, and non-sea-salt sulphate precursors in Asia and Europe. The most striking feature evident from this comparison is the very high non-sea-salt calcium in the Saharan air flow compared to all other sampled air masses. This reflects the proximity and strength of the Saharan dust sources relative to the sampling transect in the Atlantic, and that the Sahara desert is globally much the strongest source of dust to the oceans [*Jickells et al*., 2005].

We compare air masses from Pacific Zones B and C with, respectively, air masses that spent at least 5 days over the remote North (NAtl-Rem) and South (SAtl-Rem) Atlantic, assuming that these had similar histories of terrestrial contamination and aging over the ocean. Nitrate concentrations were comparable in our Zone B and C samples to those in SAtl-Rem samples, but lower than those of NAtl-Rem samples. This may be partly due to the much longer oceanic transport pathways for the Pacific samples. Ammonium concentrations in the remote South Atlantic were somewhat lower than observed in Zones B and C and ammonium concentrations in the remote Pacific were approximately double those of nitrate (Table 3). Dust concentrations (represented by nss-Ca^{2+}) were lower in zone B and C samples than in their equivalent remote air masses over the Atlantic. Non-sea-salt sulphate concentrations in zones B and C were comparable to those observed over the remote North Atlantic, but higher than over the remote South Atlantic.

4.5. Influence of Aerosol Chemical Composition on Ocean Biogeochemistry

We now attempt to estimate the impacts of atmospheric deposition on the western Pacific. Our approach is similar to that used by us in the Atlantic [*Baker et al*., 2003] and that employed recently for global scale estimates of the impacts of atmospheric deposition [*Duce et al*., 2008; *Okin et al*., 2011]. We will make these calculations for the area B, approximately 0–15°N and 150–180°E. This is the region for which we have the most data, but because aerosol concentrations and surface water nutrient (and P*, see below) status in zone C are very similar to zone B, this analysis is appropriate for zone C as well.

The Pacific aerosol results we report suggest N:P ratios vastly in excess of the ratio required by phytoplankton (the Redfield ratio of ~16:1 on a molar basis). A similar situation has also been reported for the Atlantic [*Baker et al*., 2003] and is apparently prevalent across all the world oceans [*Okin et al*., 2011]. The entire Pacific region considered here is characterized by low nitrate concentration surface waters according to the criteria used by *Duce et al*. [2008] and *Okin et al*. [2011], with average nitrate concentrations $<4\ \mu mol\ l^{-1}$, and, indeed. concentrations are generally $<1\ \mu mol\ L^{-1}$ ([*Levitus*, 1982; *Levitus*, 2010] also see http://iridl.ldeo.columbia.edu/SOURCES/.LEVITUS94/ accessed July 2013). Based on the P* (excess P with respect to N compared to Redfield ratio) mapping approach [see *Deutsch et al*., 2007; *Key et al*., 2004; *Ward et al*., 2013] all the ocean waters in zone B have rather small values of P* (about 0.1 $\mu mol\ L^{-1}$ in Zone B and 0.2 $\mu mol\ L^{-1}$ in zone C) which are similar to those seen in the North Atlantic, indicating that surface water P concentrations are low with a small excess relative to N. The waters are SPD (surplus phosphate with diazotrophs) in the new classification of *Ward et al*. [2013].

We therefore assume that the receiving ocean waters in this western Pacific region are N limited, consistent with the assumptions of others [*Okin et al*., 2011; *Dutkiewicz et al*., 2012]. Direct nutrient addition experiments in this region also suggest that primary production is limited by macronutrient supply in the West Pacific, although the addition of iron can also stimulate diatom growth in a community that is otherwise dominated by small phytoplankton [*Ditullio et al*., 1993]. This assumption of N limitation requires that water column sources can supply enough phosphorus to utilize the atmospherically delivered iron and, in the case of nonnitrogen fixers, such as picoprokaryotes, atmospherically delivered nitrogen and iron. The nitrogen supply from the atmosphere includes both nitrate and ammonium and some phytoplankton species such as

Table 5. Atmospheric Deposition Estimation for Zone B

Species	C_A (nmol m^{-3})	% Fine Mode	v_d[a] (mm s^{-1})	F^D (μmol m^{-2} d^{-1})	S	C_R (μmol kg^{-1})	F^W (μmol m^{-2} d^{-1})	F^T[b] (μmol m^{-2} d^{-1})	% Wet
NO_3^-	2.9	16	17	4.3	358	0.9	3.6	7.9	46
NH_4^+	7.1	75	5.8	3.5	240	1.5	6.0	9.5	63
WSON	4.3	45	11.5	4.2	305	1.1	4.4	8.6	51
Total N				12			14	26	54
SIP	0.022	45	11.5	0.020	305	0.006	0.024	0.043	56
Dust	1.9[c]	45	11.5	1.9[d]	305	0.5[e]	2.0[d]	3.9[d]	51
Soluble Fe				0.06[f]			0.175[g]	0.24	73

[a]Weighted deposition velocity = (fine fraction × 1 + coarse fraction × 20) mm s^{-1}.
[b]Sum of dry and wet depositions.
[c]μg m^{-3}
[d]mg m^{-2} d^{-1}.
[e]mg kg^{-1}.
[f]Assuming Fe is 3.5% of dust mass and has a solubility of 5%.
[g]Assuming Fe is 3.5% of dust mass and has a solubility of 14%.

Prochlorococcus cannot readily utilize nitrate [*Moore et al*., 2002] and so the proportions of the N species supplied may have some biogeochemical consequences. We note that the mechanisms of efficient surface water phosphorus supply to sustain positive values of P* are currently uncertain [e.g., *Mills and Arrigo*, 2010; *Moore et al*., 2009; *Monteiro and Follows*, 2012; *Palter et al*., 2011; *Ward et al*., 2013], although *Palter et al*. [2011] have demonstrated that P transport from the margins into the gyre may be the dominant source in the North Atlantic. Thus, P* represents a quasi-steady-state controlled by supply and utilization of P.

We also assume that nitrogen fixation rates are iron limited in this region consistent with the assumptions of others [*Okin et al*., 2011; *Dutkiewicz et al*., 2012; *Ward et al*., 2013]. Nitrogen fixation is potentially inhibited by the presence of dissolved nitrate or ammonium in the water column, but only at relatively high concentrations of ~10 μmol L^{-1} [*Duce et al*., 2008], with little or no inhibition at concentrations < 1 μmol L^{-1} [*Holl and Montoya*, 2005], i.e., much higher concentrations than found in these West Pacific surface waters (see earlier). Individual atmospheric deposition events will probably not push the surface waters across this surface water nitrate and ammonium concentration threshold because, based on the data in Table 5 and assuming a minimum surface mixed layer depth of 10 m, the impact of daily nitrogen deposition will on average increase surface water nitrate + ammonium concentrations by only about 3 nmol L^{-1}.

To assess the impact of atmospheric deposition, we first calculate atmospheric deposition fluxes using the approach detailed in the methods [*Baker et al*., 2003]. The results are presented in Table 5. The nitrogen deposition estimates are similar to those of others [*Duce et al*., 2008; *Jung et al*., 2011] and the dust deposition model estimates for this region [*Jickells et al*., 2005]. Our calculations suggest that wet and dry depositions are approximately comparable for total nitrogen, with all three nitrogen components contributing approximately equally, reflecting the importance of the faster deposition of coarse mode components particularly nitrate, despite their lower concentrations, as noted previously [*Jung et al*., 2011]. For dust deposition, wet and dry deposition rates are comparable, but wet deposition dominates the supply of soluble iron because of the estimated higher solubility of iron in wet deposition. The uncertainties in the parameterization of deposition rates and of iron solubility dominate the uncertainties in these calculations.

To estimate the impact of this deposition on ocean primary productivity (Box 1) we use a similar approach to that of *Baker et al*. [2003, 2007] and *Okin et al*. [2011]. We first estimate the magnitude of primary productivity that can be sustained by the atmospheric nitrogen deposition and multiply this by the Redfield C:N molar ratio of 6.6:1. We assume all of the atmospheric aerosol nitrogen is bioavailable, although we note that the bioavailability of WSON is very uncertain [*Seitzinger and Sanders*, 1999; *Cape et al*., 2011]. We then estimate the iron requirement associated with this atmospheric nitrogen fuelled productivity using a molar C:Fe ratio of 7×10^5 [*Okin et al*., 2011, and references therein], and consistent with *Boyd and Ellwood* [2010]. We subtract these iron requirements from the atmospheric iron supply to estimate the residual atmospheric iron supply. We then assume that this residual atmospheric iron supply can stimulate nitrogen fixation, and that much of the nitrogen fixed is subsequently released, probably as DON [*Mulholland*, 2007], which is assumed here to become available for nonnitrogen fixing primary producers [*Sohm et al*., 2011]. The principles and outcome of these calculations is summarized in Figure 5.

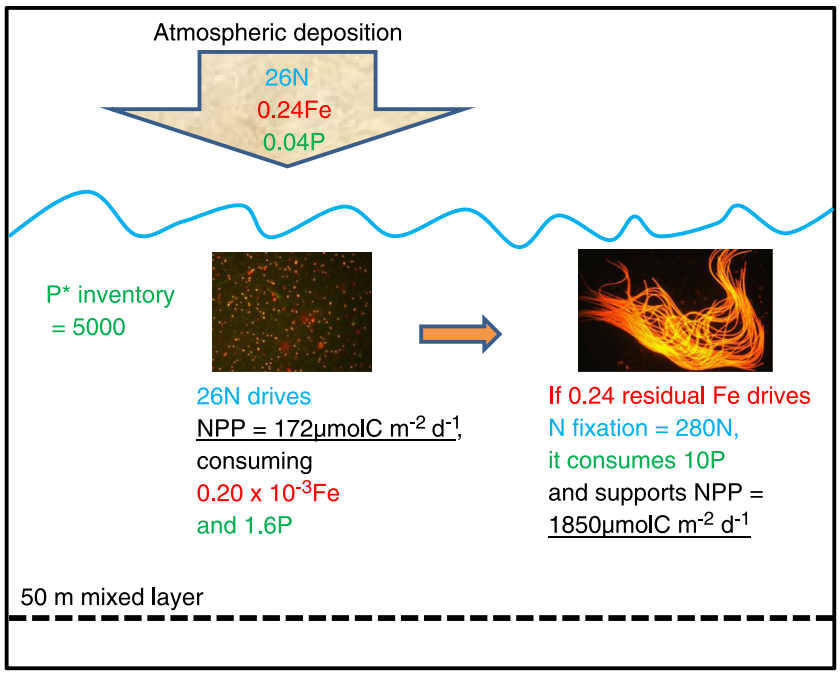

Figure 5. Summary of calculated impacts of atmospheric deposition of nitrogen (blue), iron (red), and phosphorus (green) on water column net primary production (NPP) (all rates are in μmol m^{-2} d^{-1}) with a water column P* of 0.1 μmol l^{-1}, and hence P* inventory (P*) in μmol m^{-2} for a 50 m surface mixed layer. See text for details.

Box 1. Impact of Atmospheric Deposition on the western Pacific Ocean

Total atmospheric N deposition of 26 μmol m^{-2} d^{-1} stimulates new primary production rates of 172 μmol C m^{-2} d^{-1}, assuming Redfield stoichiometry.
This deposition will require 0.25 nmol Fe m^{-2} d^{-1}, which is ~0.1% of the calculated soluble iron supply.
The residual soluble atmospheric iron supply can then sustain nitrogen fixation, and we estimate this by multiplying the atmospheric soluble iron supply by N:Fe ratios of 1333 to estimate the potential amount of nitrogen fixation that could be stimulated by the atmospheric deposition at 280 μmol m^{-2} d^{-1}.
If this fixed nitrogen is then utilized for primary production with Redfield stoichiometry, the estimated stimulated new primary production is 1848 μmol C m^{-2} d^{-1}.

We estimate nitrogen fixation rates based on our estimated residual iron supply rate and the N:Fe ratio reported for *Trichodesmium*, as discussed below. *Trichodesmium* is only one of many nitrogen-fixing organisms in ocean waters [*Moisander et al.*, 2010; *Zehr et al.*, 2008], but it is probably the best characterized [*Mahaffey et al.*, 2005] and so we choose here to use its elemental composition in subsequent calculations. As noted previously [*Baker et al.*, 2007], the iron requirements of nitrogen-fixing phytoplankton are known to be higher than other photosynthetic phytoplankton due to the iron-rich nitrogenase enzyme used for nitrogen fixation but otherwise are very poorly constrained. To convert iron supply to nitrogen fixation rates we use published N:Fe (or Fe:C and C:N) ratios for *Trichodesmium* reported by various authors as discussed below. We note the large variability in these reported ratios reflecting, at least in part, variations in iron availability which has been shown to influence *Trichodesmium* N:Fe ratios [*Berman-Frank et al.*, 2001], with the potential for these organisms to engage in luxury iron uptake [*Chen et al.*, 2011]. Our approach probably represents an upper bound of estimated nitrogen fixation rates, since these may be limited by environmental factors other than iron supply and also because some of the products of nitrogen fixation such as diatom-diazotroph assemblages may be exported to depth, and hence not utilized by phytoplankton in surface waters [*Mulholland*, 2007].

The N:Fe ratio in *Trichodesmium* is a key term in this calculation and is very uncertain. Estimates of N:Fe derived from laboratory and field measurements vary by around an order of magnitude (~400–4000 mol mol^{-1}), as discussed by *Baker et al.* [2007]. This range of reported Fe:N ratios may reflect uncertainties in measurements

and/or real environmental variability since the ratio is known to vary systematically, for instance, with iron concentrations. Recently N:Fe ratios have been estimated from an optimized fit of a global biogeochemistry model at 1333 mol mol^{-1} for a model based on *Trichodesmium* (and arguing that including other nitrogen-fixing organisms within the model did not require a significantly different ratio) [*Monteiro et al*., 2010]. We note also that it is now clear that even the Redfield ratio itself is not constant but rather varies systematically in surface waters between ocean provinces [*Martiny et al*., 2013].

The global model N:Fe estimate [*Monteiro et al*., 2010] falls between the values reported by field and laboratory studies and may represent a plausible long-term large-scale average value for the oceans. We therefore utilize the Monteiro et al. ratio in subsequent calculations, noting that there is an uncertainty of at least threefold around this value based on a comparison to the laboratory and field data. The results of this calculation are presented in Box 1. Our estimated rates of nitrogen supply from nitrogen fixation are of the same order as the measured nitrogen fixation rates of *Kitajima et al*. [2009] for this region and at the upper bound of other published estimates [e.g., *Capone*, 2001; *Montoya et al*., 2004; *Moore et al*., 2009], although recent work suggests that some published estimates of nitrogen fixation rates may be underestimated due to methodological issues [*Grosskopf et al*., 2012].

In this calculation we assume that all residual atmospheric iron supply, in excess of that required by phytoplankton growth stimulated by atmospheric nitrogen supply, is available for nitrogen fixation. However, the primary production in this region associated with other nutrient sources, such as supply from underlying waters, will also require an iron supply and this will be met in part from the atmospheric dust supply. We can estimate an upper limit on this iron requirement from the estimated rates of primary production in this area of 20 mmol C m^{-2} d^{-1} [*Antoine et al*., 1996; *Behrenfeld et al*., 2009] and the phytoplankton C:Fe ratio of 7×10^5 noted earlier, assuming that the entire iron requirement is met from the atmospheric supply. This yields an Fe requirement for primary production of 29 nmol Fe m^{-2} d^{-1}, equivalent to 12% of the atmospheric iron supply, and this suggests that the estimates of nitrogen fixation in Box 1 would be overestimated by 12%, which is small compared to the other uncertainties.

The results in Box 1 and Figure 5 suggest that the main impact of atmospheric deposition in the western Pacific on primary production is via stimulation of nitrogen fixation, rather than by direct stimulation of nondiazotrophic phytoplankton. The atmospheric iron supply allows marine diazotrophs to utilize the surface water P* leading to nitrogen fixation and ultimately enhance primary production by the whole euphotic zone community. The overall primary productivity stimulated by atmospheric deposition of N and Fe is estimated to be 1.8 mmol C m^{-2} d^{-1} (Box 1). This can be compared with estimates of primary production for this region of the order of 20 mmol C m^{-2} d^{-1} [*Behrenfeld et al*., 2009; *Antoine et al*., 1996], and estimates of global "new" production (that sustained by nutrient sources from outside the euphotic zone) which are of the order of 20% of total primary production in oligotrophic waters [*Laws et al*., 2000]. Such calculations therefore suggest that atmospheric nutrient delivery may be a very significant contribution to new primary production, and that a potentially important route for such impacts is via the stimulation of nitrogen fixation by iron deposition.

These conclusions, based on direct estimates of atmospheric deposition fluxes scaled to primary productivity by phytoplankton stoichiometry, are consistent with recent model simulations for the tropical Pacific [*Dutkiewicz et al*., 2012; *Ward et al*., 2013], and the tropical Atlantic [*Ye et al*., 2012], and measurements of nitrogen fixation rates in the region [*Kitajima et al*., 2009]. The results are also consistent with the classification of biogeochemical provinces in the Atlantic and Pacific using observed surface water stoichiometry, for instance, the P* approach. Thus, for instance, *Ward et al*. [2013]suggest, based on models and theoretical considerations, that atmospheric deposition of ~10 μmol m^{-2} yr^{-1} is required for nitrogen fixation to significantly deplete dissolved phosphorus concentrations and hence to create an SPD biogeochemical region. The atmospheric supply of soluble iron we find in the zone B and C exceeds this value, as it does in the tropical North Atlantic and our calculations using these fluxes support the conclusions of Ward et al. that the P* data for this region could arise because of atmospheric dust (iron) deposition stimulating nitrogen fixation and allowing the drawdown of excess phosphorus (P*). Based on the data in Box 1 and assuming an N/P ratio of about 28 as found in field samples [e.g., *Kustka et al*., 2003] the P* would become depleted rather slowly (400–500 days assuming no resupply).

5. Conclusions

Atmospheric nutrient deposition to the western Pacific may be responsible for about 10% of primary production and a greater fraction of export production. The atmospheric deposition is highly P deficient, and its

utilization will require consumption of some of the excess P (P*) in these waters. The atmospheric N deposition rates are small enough that they are unlikely to inhibit nitrogen fixation or to allow small nondiazotrophic phytoplankton to consume the atmospheric Fe or water column P* supply. We calculate that the main impact of atmospheric deposition on primary production is via stimulation of nitrogen fixation, although this conclusion is very sensitive to the value of N:Fe for nitrogen fixation. The dust and iron fluxes we report for the western Pacific are substantially lower than those in the tropical North Atlantic, which would suggest that the amounts of nitrogen fixation stimulated should be less, but greater than seen in the tropical South Atlantic, if atmospheric dust supply and stoichiometry is the main control on nitrogen fixation. Model estimates of dust and nutrient deposition suggest a strong gradient of decreasing atmospheric deposition moving from west to east in the South Pacific, whereas the whole tropical North Pacific appears to receive sufficient atmospheric iron to allow biogeochemically significant amounts of nitrogen fixation. Throughout this region there is a small P* excess in surface waters that is sufficient to allow the utilization of atmospheric deposition of N and Fe thereby increasing overall productivity.

Acknowledgments

This work was funded in part by NERC grant NE/F017359/1. Toyofuji Shipping Co. is acknowledged for their generous cooperation with the Ship of Opportunity program by NIES. Financial support to operate the Ship of Opportunity program by NIES was provided by Ministry of the Environment, Japan, as Global Environment Research Account for National Institutes. We thank the reviewers and Editors for their help in improving this paper.

References

Allen, A. G., and A. H. Miguel (1995), Biomass burning in the Amazon—Characterization of the ionic component of aerosols generated from flaming and smoldering rainforest and savannah, *Environ. Sci. Technol.*, *29*, 486–493.

Antoine, D., J. M. Andre, and A. Morel (1996), Oceanic primary production. 2. Estimation at global scale from satellite (coastal zone color scanner) chlorophyll, *Global Biogeochem. Cycles*, *10*, 57–69, doi:10.1029/95GB02832.

Arimoto, R., X. Y. Zhang, B. J. Huebert, C. H. Kang, D. L. Savoie, J. M. Prospero, S. K. Sage, C. A. Schloesslin, H. M. Khaing, and S. N. Oh (2004), Chemical composition of atmospheric aerosols from Zhenbeitai, China, and Gosan, South Korea, during ACE-Asia, *J. Geophys. Res.*, *109*, D19S04, doi:10.1029/2003JD004323.

Baker, A. R., and T. D. Jickells (2006), Mineral particle size as a control on aerosol iron solubility, *Geophys. Res. Lett.*, *33*, L17608, doi:10.1029/2006GL026557.

Baker, A. R., S. D. Kelly, K. F. Biswas, M. Witt, and T. D. Jickells (2003), Atmospheric deposition of nutrients to the Atlantic Ocean, *Geophys. Res. Lett.*, *30*, 2296, doi:10.1029/2003GL018518.

Baker, A. R., T. D. Jickells, K. F. Biswas, K. Weston, and M. French (2006a), Nutrients in atmospheric aerosol particles along the Atlantic Meridional Transect, *Deep Sea Res. Part II*, *53*, 1706–1719.

Baker, A. R., T. D. Jickells, M. Witt, and K. L. Linge (2006b), Trends in the solubility of iron, aluminium, manganese and phosphorus in aerosol collected over the Atlantic Ocean, *Mar. Chem.*, *98*, 43–58.

Baker, A. R., K. Weston, S. D. Kelly, M. Voss, P. Streu, and J. N. Cape (2007), Dry and wet deposition of nutrients from the tropical Atlantic atmosphere: Links to primary productivity and nitrogen fixation, *Deep Sea Res. Part I*, *54*, 1704–1720.

Baker, A. R., T. Lesworth, C. Adams, T. D. Jickells, and L. Ganzeveld (2010), Estimation of atmospheric nutrient inputs to the Atlantic Ocean from 50°N to 50°S based on large-scale field sampling: Fixed nitrogen and dry deposition of phosphorus, *Global Biogeochem. Cycles*, *24*, GB3006, doi:10.1029/2009GB003634.

Behrenfeld, M. J., et al. (2009), Satellite-detected fluorescence reveals global physiology of ocean phytoplankton, *Biogeosciences*, *6*, 779–794.

Berman-Frank, I., J. T. Cullen, Y. Shaked, R. M. Sherrell, and P. G. Falkowski (2001), Iron availability, cellular iron quotas, and nitrogen fixation in *Trichodesmium*, *Limnol. Oceanogr.*, *46*, 1249–1260.

Boyd, P. W., and M. J. Ellwood (2010), The biogeochemical cycle of iron in the ocean, *Nat. Geosci.*, *3*, 675–682.

Boyd, P. W., D. S. Mackie, and K. A. Hunter (2010), Aerosol iron deposition to the surface ocean—Modes of iron supply and biological responses, *Mar. Chem.*, *120*, 128–143.

Cai, W. J., et al. (2012), More extreme swings of the South Pacific convergence zone due to greenhouse warming, *Nature*, *488*, 365–369.

Cape, J. N., A. Kirika, A. P. Rowland, D. R. Wilson, T. D. Jickells, and S. E. Cornell (2001), Organic nitrogen in precipitation: Real problem or sampling artefact?, *Sci. World*, *1*, 230–237.

Cape, J. N., S. E. Cornell, T. D. Jickells, and E. Nemitz (2011), Organic nitrogen in the atmosphere—Where does it come from? A review of sources and methods, *Atmos. Res.*, *102*, 30–48.

Capone, D. G. (2001), Marine nitrogen fixation: What's the fuss?, *Curr. Opin. Microbiol.*, *4*, 341–348.

Chen, H. Y., L. D. Chen, Z. Y. Chiang, C. C. Hung, F. J. Lin, W. C. Chou, G. C. Gong, and L. S. Wen (2010), Size fractionation and molecular composition of water-soluble inorganic and organic nitrogen in aerosols of a coastal environment, *J. Geophys. Res.*, *115*, D22307, doi:10.1029/2010JD014157.

Chen, Y., A. Tovar-Sanchez, R. L. Siefert, S. A. Sanudo-Wilhelmy, and G. S. Zhuang (2011), Luxury uptake of aerosol iron by *Trichodesmium* in the western tropical North Atlantic, *Geophys. Res. Lett.*, *38*, L18602, doi:10.1029/2011GL048972.

Cornell, S. E., T. D. Jickells, J. N. Cape, A. P. Rowland, and R. A. Duce (2003), Organic nitrogen deposition on land and coastal environments: A review of methods and data, *Atmos. Environ.*, *37*, 2173–2191.

Deutsch, C., J. L. Sarmiento, D. M. Sigman, N. Gruber, and J. P. Dunne (2007), Spatial coupling of nitrogen inputs and losses in the ocean, *Nature*, *445*, 163–167.

Ditullio, G. R., D. A. Hutchins, and K. W. Bruland (1993), Interaction of iron and major nutrients controls phytoplankton growth and species composition in the tropical North Pacific Ocean, *Limnol. Oceanogr.*, *38*, 495–508.

Draxler, R. R., and G. D. Rolph (2003), *HYSPLIT (HYbrid Single-Particle Lagrangian Integrated Trajectory) Model*, NOAA Air Resources Laboratory, Silver Spring, Md. [Available at http://www.arl.noaa.gov/ready/hysplit4.html.]

Duce, R. A. (1995), Sources, distributions and fluxes of mineral aerosols and their relation to climate, in *Aerosol Forcing of Climate*, edited by R. J. Charlson and J. Heintzenberg, p. 43, John Wiley, Chichester, U. K.

Duce, R. A., et al. (2008), Impacts of atmospheric anthropogenic nitrogen on the open ocean, *Science*, *320*, 893–897.

Dutkiewicz, S., B. A. Ward, F. Monteiro, and M. J. Follows (2012), Interconnection of nitrogen fixers and iron in the Pacific Ocean: Theory and numerical simulations, *Global Biogeochem. Cycles*, *26*, GB1012, doi:10.1029/2011GB004039.

Furutani, H., A. Meguro, H. Iguchi, and M. Uematsu (2010), Geographical distribution and sources of phosphorus in atmospheric aerosol over the North Pacific Ocean, *Geophys. Res. Lett.*, *37*, L03805, doi:10.1029/2009GL041367.

Galloway, J. N., D. L. Savoie, W. C. Keene, and J. M. Prospero (1993), The temporal and spatial variability of scavenging ratios for nss sulfate, nitrate, methanesulfonate and sodium in the atmosphere over the North Atlantic Ocean, *Atmos. Environ. Part A*, *27*, 235–250.
Grosskopf, T., W. Mohr, T. Baustian, H. Schunck, D. Gill, M. M. M. Kuypers, G. Lavik, R. A. Schmitz, D. W. R. Wallace, and J. Laroche (2012), Doubling of marine dinitrogen-fixation rates based on direct measurements, *Nature*, *488*, 361–364.
Holl, C. M., and J. P. Montoya (2005), Interactions between nitrate uptake and nitrogen fixation in continuous cultures of the marine diazotroph *Trichodesmium* (Cyanobacteria), *J. Phycol.*, *41*, 1178–1183.
Hsu, S. C., et al. (2010), Sources, solubility, and dry deposition of aerosol trace elements over the East China Sea, *Mar. Chem.*, *120*, 116–127.
Huebert, B. J., T. Bates, P. B. Russell, G. Y. Shi, Y. J. Kim, K. Kawamura, G. Carmichael, and T. Nakajima (2003), An overview of ACE-Asia: Strategies for quantifying the relationships between Asian aerosols and their climatic impacts, *J. Geophys. Res.*, *108*(D23), 8633, doi:10.1029/2003JD003550.
Jickells, T. D., and L. J. Spokes (2001), Atmospheric iron inputs to the oceans, in *The Biogeochemistry of Iron in Seawater*, *SCOR/IUPAC Ser.*, vol. 7, edited by D. R. Turner and K. Hunter, pp. 85–121, Wiley, New York.
Jickells, T. D., et al. (2005), Global iron connections between desert dust, ocean biogeochemistry, and climate, *Science*, *308*, 67–71.
Jung, J. Y., H. Furutani, and M. Uematsu (2011), Atmospheric inorganic nitrogen in marine aerosol and precipitation and its deposition to the North and South Pacific Oceans, *J. Atmos. Chem.*, *68*, 157–181.
Keene, W. C., A. A. P. Pszenny, J. N. Galloway, and M. E. Hawley (1986), Sea-salt corrections and interpretation of constituent ratios in marine precipitation, *J. Geophys. Res.*, *91*, 6647–6658, doi:10.1029/JD091iD06p06647.
Key, R. M., A. Kozyr, C. L. Sabine, K. Lee, R. Wanninkhof, J. L. Bullister, R. A. Feely, F. J. Millero, C. Mordy, and T. H. Peng (2004), A global ocean carbon climatology: Results from Global Data Analysis Project (GLODAP), *Global Biogeochem. Cycles*, *18*, GB4031, doi:10.1029/2004GB002247.
Kim, T. W., K. Lee, R. G. Najjar, H. D. Jeong, and H. J. Jeong (2011), Increasing N abundance in the northwestern Pacific Ocean due to atmospheric nitrogen deposition, *Science*, *334*, 505–509.
Kitajima, S., K. Furuya, F. Hashihama, S. Takeda, and J. Kanda (2009), Latitudinal distribution of diazotrophs and their nitrogen fixation in the tropical and subtropical western North Pacific, *Limnol. Oceanogr.*, *54*, 537–547.
Kline, J., B. Huebert, S. Howell, B. Blomquist, J. Zhuang, T. Bertram, and J. Carrillo (2004), Aerosol composition and size versus altitude measured from the C-130 during ACE-Asia, *J. Geophys. Res.*, *109*, D19S08, doi:10.1029/2004JD004540.
Krüger, K., and B. Quack (2013), Introduction to special issue: The TransBrom Sonne expedition in the tropical West Pacific, *Atmos. Chem. Phys.*, *13*, 9439–9446.
Kustka, A. B., S. A. Sanudo-Wilhelmy, E. J. Carpenter, D. Capone, J. Burns, and W. G. Sunda (2003), Iron requirements for dinitrogen- and ammonium-supported growth in cultures of *Trichodesmium* (IMS 101): Comparison with nitrogen fixation rates and iron carbon ratios of field populations, *Limnol. Oceanogr.*, *48*, 1869–1884.
Laws, E. A., P. G. Falkowski, W. O. Smith, H. Ducklow, and J. J. Mccarthy (2000), Temperature effects on export production in the open ocean, *Global Biogeochem. Cycles*, *14*, 1231–1246, doi:10.1029/1999GB001229.
Lesworth, T., A. R. Baker, and T. Jickells (2010), Aerosol organic nitrogen over the remote Atlantic Ocean, *Atmos. Environ.*, *44*, 1887–1893.
Levitus, S. (Ed.) (2010), *Nutrients (Phosphate, Nitrate, Silicate)*, NOAA Atlas NESDIS 71, U.S. Government Printing Office, Washington, D. C.
Levitus, S. E. (1982), *Climatological Atlas of the World Ocean*, *NOAA Professional Paper 13*, pp. 1–173, U.S. Government Printing Office, Washington, D. C.
Liu, X. J., et al. (2013), Enhanced nitrogen deposition over China, *Nature*, *494*, 459–462.
Mahaffey, C., A. F. Michaels, and D. G. Capone (2005), The conundrum of marine N-2 fixation, *Am. J. Sci.*, *305*, 546–595.
Mahowald, N., et al. (2008), The global distribution of atmospheric phosphorus deposition and anthropogenic impacts, *Global Biogeochem. Cycles*, *22*, GB4026, doi:10.1029/2008GB003240.
Martiny, A. C., C. T. Pham, F. W. Primeau, J. A. Vrugt, J. K. Moore, S. A. Levin, and M. W. Lomas (2013), Strong latitudinal patterns in the elemental ratios of marine plankton and organic matter, *Nat. Geosci.*, *6*, 279–283.
Matsumoto, K., Y. Uyama, T. Hayano, and M. Uematsu (2004), Transport and chemical transformation of anthropogenic and mineral aerosol in the marine boundary layer over the western North Pacific Ocean, *J. Geophys. Res.*, *109*, D21206, doi:10.1029/2004JD004696.
Merrill, J. (1989), Atmospheric long range transport to the Pacific ocean, in *Chemical Oceanography*, vol. 10, edited by J. P. Riley, R. Chester, and R. A. Duce, pp. 15–50, Academic, San Diego, Calif.
Merrill, J. T., R. Bleck, and L. Avila (1985), Modeling atmospheric transport to the Marshall islands, *J. Geophys. Res.*, *90*, 2927–2936.
Mills, M. M., and K. R. Arrigo (2010), Magnitude of oceanic nitrogen fixation influenced by the nutrient uptake ratio of phytoplankton, *Nat. Geosci.*, *3*, 412–416.
Mills, M. M., C. Ridame, M. Davey, J. La Roche, and R. J. Geider (2004), Iron and phosphorus co-limit nitrogen fixation in the eastern tropical North Atlantic, *Nature*, *429*, 292–294.
Miyazaki, Y., K. Kawamura, and M. Sawano (2010), Size distributions of organic nitrogen and carbon in remote marine aerosols: Evidence of marine biological origin based on their isotopic ratios, *Geophys. Res. Lett.*, *37*, L06803, doi:10.1029/2010GL042483.
Miyazaki, Y., K. Kawamura, J. Jung, H. Furutani, and M. Uematsu (2011), Latitudinal distributions of organic nitrogen and organic carbon in marine aerosols over the western North Pacific, *Atmos. Chem. Phys.*, *11*, 3037–3049.
Moffet, R. C., H. Furutani, T. C. Roedel, T. R. Henn, P. O. Sprau, A. Laskin, M. Uematsu, and M. K. Gilles (2012), Iron speciation and mixing in single aerosol particles from the Asian continental outflow, *J. Geophys. Res.*, *117*, D07204, doi:10.1029/2011JD016746.
Moisander, P. H., R. A. Beinart, I. Hewson, A. E. White, K. S. Johnson, C. A. Carlson, J. P. Montoya, and J. P. Zehr (2010), Unicellular cyanobacterial distributions broaden the oceanic N-2 fixation domain, *Science*, *327*, 1512–1514.
Monteiro, F. M., and M. J. Follows (2012), On nitrogen fixation and preferential remineralization of phosphorus, *Geophys. Res. Lett.*, *39*, L06607, doi:10.1029/2012GL050897.
Monteiro, F. M., M. J. Follows, and S. Dutkiewicz (2010), Distribution of diverse nitrogen fixers in the global ocean, *Global Biogeochem. Cycles*, *24*, GB3017, doi:10.1029/2009GB003731.
Montoya, J. P., C. M. Holl, J. P. Zehr, A. Hansen, T. A. Villareal, and D. G. Capone (2004), High rates of N2 fixation by unicellular diazotrophs in the oligotrophic Pacific Ocean, *Nature*, *430*, 1027–1031.
Moore, C. M., et al. (2009), Large-scale distribution of Atlantic nitrogen fixation controlled by iron availability, *Nat. Geosci.*, *2*, 867–871.
Moore, C. M., et al. (2013), Processes and patterns of oceanic nutrient limitation, *Nat. Geosci.*, *6*, 701–710, doi:10.1038/ngeo1765.
Moore, L. R., A. F. Post, G. Rocap, and S. W. Chisholm (2002), Utilization of different nitrogen sources by the marine cyanobacteria *Prochlorococcus* and *Synechococcus*, *Limnol. Oceanogr.*, *47*, 989–996.
Mulholland, M. R. (2007), The fate of nitrogen fixed by diazotrophs in the ocean, *Biogeosciences*, *4*, 37–51.
Nakamura, T., H. Ogawa, D. K. Maripi, and M. Uematsu (2006), Contribution of water soluble organic nitrogen to total nitrogen in marine aerosols over the East China Sea and western North Pacific, *Atmos. Environ.*, *40*, 7259–7264.

Nara, H., H. Tanimoto, Y. Nojiri, H. Mukai, J. Y. Zeng, Y. Tohjima, and T. Machida (2011), CO emissions from biomass burning in South-east Asia in the 2006 El Niño year: Shipboard and AIRS satellite observations, *Environ. Chem.*, *8*, 213–223.

Natsagdorj, L., D. Jugder, and Y. S. Chung (2003), Analysis of dust storms observed in Mongolia during 1937–1999, *Atmos. Environ.*, *37*, 1401–1411.

Okin, G., et al. (2011), Impacts of atmospheric nutrient deposition on marine productivity: Roles of nitrogen, phosphorus, and iron, *Global Biogeochem. Cycles*, *25*, GB2022, doi:10.1029/2010GB003858.

Ooki, A., M. Uematsu, and S. Noriki (2007), Size-resolved sulfate and ammonium measurements in marine boundary layer over the North and South Pacific, *Atmos. Environ.*, *41*, 81–91.

Palter, J. B., M. S. Lozier, J. L. Sarmiento, and R. G. Williams (2011), The supply of excess phosphate across the Gulf Stream and the maintenance of subtropical nitrogen fixation, *Global Biogeochem. Cycles*, *25*, GB4007, doi:10.1029/2010GB003955.

Prospero, J. M., M. Uematsu, and D. L. Savoie (1989), Mineral aerosol transport to the Pacific Ocean, in *SEAREX: The Sea/Air Exchange*, *Chemical Oceanography*, vol. 10, edited by J. P. Riley, R. Chester, and R. A. Duce, pp. 187–218, Academic Press, New York.

Revel-Rolland, M., P. De Deckker, B. Delmonte, P. P. Hesse, J. W. Magee, I. Basile-Doelsch, F. Grousset, and D. Bosch (2006), Eastern Australia: A possible source of dust in East Antarctica interglacial ice, *Earth Planet. Sci. Lett.*, *249*, 1–13.

Savoie, D. L., and J. M. Prospero (1980), Water-soluble potassium, calcium, and magnesium in the aerosols over the tropical North Atlantic, *J. Geophys. Res.*, *85*, 385–392, doi:10.1029/JC085iC01p00385.

Savoie, D. L., J. M. Prospero, J. T. Merrill, and M. Uematsu (1989), Nitrate in the atmospheric boundary-layer of the tropical South-Pacific—Implications regarding sources and transport, *J. Atmos. Chem.*, *8*, 391–415.

Seitzinger, S. P., and R. W. Sanders (1999), Atmospheric inputs of dissolved organic nitrogen stimulate estuarine bacteria and phytoplankton, *Limnol. Oceanogr.*, *44*, 721–730.

Sholkovitz, E. R., P. N. Sedwick, T. M. Church, A. R. Baker, and C. F. Powell (2012), Fractional solubility of aerosol iron: Synthesis of a global-scale data set, *Geochim. Cosmochim. Acta*, *89*, 173–189.

Sohm, J. A., E. A. Webb, and D. G. Capone (2011), Emerging patterns of marine nitrogen fixation, *Nat. Rev. Microbiol.*, *9*, 499–508.

Somes, C. J., A. Schmittner, and M. A. Altabet (2010), Nitrogen isotope simulations show the importance of atmospheric iron deposition for nitrogen fixation across the Pacific Ocean, *Geophys. Res. Lett.*, *37*, L23605, doi:10.1029/2010GL044537.

Song, S. K., Y. K. Kim, Z. H. Shon, and H. W. Lee (2008), Influence of meteorological conditions on trans-Pacific transport of Asian dust during spring season, *J. Aerosol Sci.*, *39*, 1003–1017.

Srinivas, B., and M. M. Sarin (2012), Atmospheric pathways of phosphorous to the Bay of Bengal: Contribution from anthropogenic sources and mineral dust, *Tellus B*, *64*, 17,174.

Stumm, W., and J. J. Morgan (1996), *Aquatic Chemistry. Chemical Equilibria and Rates in Natural Waters*, 3rd ed., Wiley, New York.

Suzuki, T., and S. Tsunogai (1988), Origin of calcium in aerosols over the western North Pacific, *J. Atmos. Chem.*, *6*, 363–374.

Tsunogai, S., and T. Kondo (1982), Sporadic transport and deposition of continental aerosols to the Pacific Ocean, *J. Geophys. Res.*, *87*, 8870–8874, doi:10.1029/JC087iC11p08870.

Tsunogai, S., T. Suzuki, T. Kurata, and M. Uematsu (1985), Seasonal and areal variation of continental aerosol in the surface air over the western North Pacific region, *J. Oceanogr. Soc. Jpn.*, *41*, 427–434.

Uematsu, M., R. A. Duce, J. M. Prospero, L. Chen, J. T. Merrill, and R. L. Mcdonald (1983), Transport of mineral aerosol from Asia over the North Pacific Ocean, *J. Geophys. Res.*, *88*, 5343–5352, doi:10.1029/JC088iC09p05343.

Uematsu, M., Z. F. Wang, and I. Uno (2003), Atmospheric input of mineral dust to the western North Pacific region based on direct measurements and a regional chemical transport model, *Geophys. Res. Lett.*, *30*(6), 1342, doi:10.1029/2002GL016645.

Uematsu, M., M. Toratani, M. Kajino, Y. Narita, Y. Senga, and T. Kimoto (2004), Enhancement of primary productivity in the western North Pacific caused by the eruption of the Miyake-jima Volcano, *Geophys. Res. Lett.*, *31*, L06106, doi:10.1029/2003GL018790.

Uematsu, M., H. Hattori, T. Nakamura, Y. Narita, J. Jung, K. Matsumoto, Y. Nakaguchi, and M. D. Kumar (2010), Atmospheric transport and deposition of anthropogenic substances from the Asia to the East China Sea, *Mar. Chem.*, *120*, 108–115.

Wagener, T., C. Guieu, R. Losno, S. Bonnet, and N. Mahowald (2008), Revisiting atmospheric dust export to the Southern Hemisphere ocean: Biogeochemical implications, *Global Biogeochem. Cycles*, *22*, GB2006, doi:10.1029/2007GB002984.

Ward, B. A., S. Dutkiewicz, C. M. Moore, and M. J. Follows (2013), Iron, phosphorus, and nitrogen supply ratios define the biogeography of nitrogen fixation, *Limnol. Oceanogr.*, *58*, 2059–2075.

Xie, P. P., and P. A. Arkin (1997), Global precipitation: A 17-year monthly analysis based on gauge observations, satellite estimates, and numerical model outputs, *Bull. Am. Meteorol. Soc.*, *78*, 2539–2558.

Xuan, J., and I. N. Sokolik (2002), Characterization of sources and emission rates of mineral dust in Northern China, *Atmos. Environ.*, *36*, 4863–4876.

Ye, Y., C. Volker, A. Bracher, B. Taylor, and D. A. Wolf-Gladrow (2012), Environmental controls on N-2 fixation by *Trichodesmium* in the tropical eastern North Atlantic Ocean—A model-based study, *Deep Sea Res. Part I*, *64*, 104–117.

Yeatman, S. G., L. J. Spokes, and T. D. Jickells (2001), Comparisons of coarse-mode aerosol nitrate and ammonium at two polluted coastal sites, *Atmos. Environ.*, *35*, 1321–1335.

Zehr, J. P., S. R. Bench, B. J. Carter, I. Hewson, F. Niazi, T. Shi, H. J. Tripp, and J. P. Affourtit (2008), Globally distributed uncultivated oceanic N(2)-fixing cyanobacteria lack oxygenic photosystem II, *Science*, *322*, 1110–1112.

Zhang, J., G. S. Zhang, Y. F. Bi, and S. M. Liu (2011), Nitrogen species in rainwater and aerosols of the Yellow and East China seas: Effects of the East Asian monsoon and anthropogenic emissions and relevance for the NW Pacific Ocean, *Global Biogeochem. Cycles*, *25*, GB3020, doi:10.1029/2010GB003896.

Zhang, Q., et al. (2007), NO_x emission trends for China, 1995–2004: The view from the ground and the view from space, *J. Geophys. Res.*, *112*, D22306, doi:10.1029/2007JD008684.

Zhou, M. Y., N. P. Lu, J. Miller, F. P. Parungo, C. Nagamoto, and S. J. Yang (1992), Characterization of atmospheric aerosols and of suspended particles in seawater in the Western Pacific Ocean, *J. Geophys. Res.*, *97*, 7553–7567, doi:10.1029/92JD00507.